

Energy Analysis of Metal-Ligand Bonding in Transition Metal Complexes with Terminal Group-13 Diyl Ligands (CO)₄Fe-ER, Fe(EMe)₅ and Ni(EMe)₄ (E = B–Tl; R = Cp, N(SiH₃)₂, Ph, Me) Reveals Significant π Bonding in Homoleptical Molecules[‡]

Jamal Uddin[†] and Gernot Frenking*

Contribution from the Fachbereich Chemie, Philipps-Universität, Hans-Meerwein-Strasse, D-35032 Marburg, Germany.

Received August 1, 2000. Revised Manuscript Received November 27, 2000

Abstract: The metal-ligand bonds of the title compounds have been investigated with the help of an energy partitioning analysis at the DFT level. It was found that the attractive orbital interactions between Fe and ER in (CO)₄Fe-ER arise mainly from Fe ← ER σ donation. Only the boron diyl complexes (CO)₄Fe-BR have significant contributions by Fe → ER π back-donation, but the Fe ← BR σ -donation remains the dominant orbital interaction term. The relative contributions of Fe-ER σ donation and π back-donation are only slightly altered when R changes from a good π donor to a poor π donor. Electrostatic forces between the metal fragment and the diyl ligand are always attractive, and they are very strong. They arise from the attraction between the local negative charge concentration at the overall positively charged donor atom E of the Lewis base ER and the positive charge of the iron nucleus. Electrostatic interactions and covalent interactions in (CO)₄Fe-ER complexes have a similar strength when E is Al–Tl and when R is a good π donor substituent. The Fe-BR bonds of the boron carbonyldiyl complexes have a significantly higher ionic character than the heavier group-13 analogues. Weak π donor substituents R enhance the ionic character of the (CO)₄Fe-ER bond. The metal-ligand bonds in the homoleptic complexes Fe(EMe)₅ and Ni(EMe)₄ have a higher ionic character than in (CO)₄Fe-ER. The contribution of the TM → ER π back-donation to the ΔE_{orb} term becomes clearly higher and contributes significantly to the total orbital interactions in the homoleptic complexes where no other π acceptor ligands are present. The ligand BMe is nearly as strong a π acceptor in Fe(BMe)₅ as CO is in Fe(CO)₅.

1. Introduction

The coordination chemistry of transition metal (TM) complexes with group-13 diyl ligands ER (E = B–Tl), which was fueled by the successful syntheses of numerous compounds L_n-TM-ER where the elements E have the formal oxidation state 1+,^{1–9} has blossomed in the last five years. The geometries of many complexes could for the first time be determined by X-ray

structure analysis, which makes it possible to unequivocally identify their atomic connectivity. Contrary to the clear information about the geometries of the molecules, the discussion about the bonding situation between the transition metal and the diyl ligand ER has not come to a generally accepted understanding of the nature of the chemical bond.

Two questions are at the center of the discussion. One question addresses the degree of covalent and ionic character of the TM-ER bonds. The second question concerns the extent of the TM → ER π back-bonding contribution to the metal-ligand orbital interactions (Figure 1a). Most complexes with diyl ligands ER which could become isolated so far either have strong π donor substituents R, or the ligand ER is stabilized by bidentate Lewis bases.¹ This finding led to the suggestion that the covalent contributions to the TM-ER bonds mainly arise from TM ← ER σ donation and that the TM → ER π back-donation is much less important. Inspection of the charge

[†] Present address: Department of Chemistry, University of Wisconsin, Madison, WI 53705.

[‡] Theoretical Studies of Inorganic Compounds, Part XII. Part XI: Gigu, K.; Bickelhaupt, M. F.; Frenking, G. *Inorg. Chem.* **2000**, *39*, 4776.

(1) Reviews: (a) Irvine, G. J.; Lesley, M. J. G.; Marder, T. B.; Norman, N. C.; Rice, C. R.; Robins, E. G.; Roper, W. R.; Whittell, G. R.; Wright, L. J. *Chem. Rev.* **1998**, *98*, 2685. (b) Braunschweig, H. *Angew. Chem.* **1998**, *110*, 1882; *Angew. Chem., Int. Ed. Engl.* **1998**, *37*, 1786. (c) Wrackmeyer, B. *Angew. Chem.* **1999**, *111*, 817; *Angew. Chem., Int. Ed. Engl.* **1999**, *38*, 771. (d) Fischer, R. A.; Weiß, J. *Angew. Chem.* **1999**, *111*, 3002; *Angew. Chem., Int. Ed. Engl.* **1999**, *38*, 2830.

(2) (a) Schulte, M. M.; Herdtweck, E.; Randaschl-Sieber, G.; Fischer, R. A. *Angew. Chem.* **1996**, *108*, 489; *Angew. Chem., Int. Ed. Engl.* **1996**, *35*, 424. (b) Weiß, J.; Stetzkamp, D.; Nuber, B.; Fischer, R. A.; Boehme, C.; Frenking, G. *Angew. Chem.* **1997**, *109*, 95; *Angew. Chem., Int. Ed. Engl.* **1997**, *36*, 70. (c) Fischer, R. A.; Schulte, M. M.; Weiss, J.; Zsolnai, L.; Jacobi, A.; Huttner, G.; Frenking, G.; Boehme, C.; Vyboishchikov, S. F. *J. Am. Chem. Soc.* **1998**, *120*, 1237. (d) Weiss, D.; Steinke, T.; Winter, M.; Fischer, R. A.; Fröhlich, N.; Uddin, J.; Frenking, G. *Organometallics* **2000**, *19*, 4583.

(3) (a) Uhl, W.; Pohlmann, M.; Wartchow, R. *Angew. Chem.* **1998**, *110*, 1007; *Angew. Chem., Int. Ed. Engl.* **1998**, *37*, 961. (b) Frenking, G.; Uddin, J.; Uhl, W.; Benter, M.; Melle, S.; Saak, W. *Organometallics* **1999**, *18*, 3778.

(4) Cowley, A. H.; Lomeli, V.; Voigt, A. *J. Am. Chem. Soc.* **1998**, *120*, 6401.

(5) Braunschweig, H.; Kollann, C.; Englert, U. *Angew. Chem.* **1998**, *110*, 3355; *Angew. Chem., Int. Ed. Engl.* **1998**, *37*, 3179.

(6) Su, J.; Li, X.-W.; Crittendon, R. C.; Campana, C. F.; Robinson, G. H. *Organometallics* **1997**, *16*, 4511.

(7) Haubrich, S. T.; Power, P. P. *J. Am. Chem. Soc.* **1998**, *120*, 2202.

(8) Yu, Q.; Purath, A.; Donchev, A.; Schnöckel, H. *J. Organomet. Chem.* **1999**, *584*, 94.

(9) (a) Jutzi, P.; Neumann, B.; Reumann, G.; Stämmler, H.-G. *Organometallics* **1998**, *17*, 1305. (b) Jutzi, P.; Neumann, B.; Reumann, G.; Schebaum, L. O.; Stämmler, H.-G. *Organometallics* **1999**, *18*, 2550.

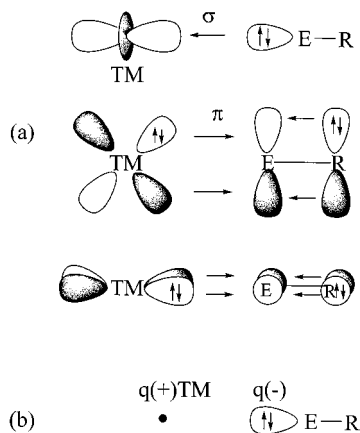


Figure 1. (a) Schematic representation of the TM-ER orbital interactions when R has occupied $p(\pi)$ orbitals. (b) Schematic representation of the dominant electrostatic interactions between the local electronic charge concentration at the donor atom E and the nucleus of the acceptor atom Fe. Note that E has an overall positive partial charge and the Fe atom has an overall negative partial charge.

donation and back-donation in TM complexes with ligands ECp showed that the $\text{TM} \leftarrow \text{ECp} \sigma$ donation is, indeed, much bigger than the $\text{TM} \rightarrow \text{ECp} \pi$ back-donation.^{2b,c} It was also shown, however, that the latter interaction becomes stronger in complexes with ligands ER where R is H, Cl.^{2c}

The successful isolation of $(\text{CO})_4\text{Fe-GaAr}^*$ ($\text{Ar}^* = 2,6\text{-}(2,4,6\text{-triiisopropylphenyl})\text{-phenyl}$)⁶ and the syntheses of the first homoleptic diyl complexes $\text{Ni}(\text{E-C}(\text{SiMe}_3)_3)_4$ when E is In^{3a} and Ga^{3b} gave rise to the speculation that $\text{TM} \rightarrow \text{ER} \pi$ back-donation may become significant when R is not a π donor. A theoretical study by Cotton and Feng¹⁰ challenged the suggestion⁶ that $\text{Fe} \rightarrow \text{Ar}^* \pi$ back-donation makes a significant contribution to the bonding in $(\text{CO})_4\text{Fe-GaAr}^*$. Other theoretical studies of the electronic structure of group-13 diyl complexes $\text{L}_n\text{TM-ER}$ showed, however, that the $p(\pi)$ AOs of E are clearly stronger populated in the complexes than in the free ligands ER when R is Ph or Me.¹¹ The insight into the bonding situation of the compounds which was gained from theoretical studies has recently been reviewed.¹²

The nature of the iron-group-13-element bonding in diyl complexes $(\text{CO})_4\text{Fe-ER}$ was addressed in a very recent theoretical study by Macdonald and Cowley (MC).¹³ This paper reported for the first time not only a decomposition of the electronic charge distribution in the complexes with the substituents R being Cp, Me, and $\text{N}(\text{SiH}_3)_2$, it also gave the results of an energy partitioning of the metal-ligand bonding in terms of orbital interactions, Pauli repulsion, and electrostatic interactions. Knowledge about the different energy contributions to the TM-ER interactions is more relevant than previous results that were obtained from population analyses,^{3b,8,10-12} because the relative size of a charge term does not necessarily correlate with the strength of the associated energy contribution. Unfortunately, the bonding analysis reported by MC¹³ did not give the pivotal information about the interaction terms which is available from the energy partitioning scheme, although the results are highly relevant in order to answer the question about the nature of the TM-ER bonding interactions. Two important pieces of informa-

tion are missing in the paper. One missing piece is the breakdown of the attractive orbital interaction term ΔE_{orb} into contributions that arise from orbitals which have σ and π symmetry. The second missing piece is the individual contributions by the Pauli repulsion ΔE_{Pauli} and the electrostatic interaction ΔE_{elstat} . MC gave only the sum of $\Delta E_{\text{Pauli}} + \Delta E_{\text{elstat}} = \Delta E^\circ$. A detailed bonding analysis of $\text{Cr}(\text{CO})_6$ by Davidson¹⁴ and a recent theoretical study of the isoelectronic hexacarbonyls $\text{TM}^q(\text{CO})_6$ when TM^q is Hf^{2-} , Ta^- , W, Re^+ , Os^{2+} , and Ir^{3+} by us showed that the Pauli repulsion and the electrostatic interactions must explicitly be considered in order to fully understand the bonding interactions.¹⁵

From the reported data of MC,¹³ it is, thus, not possible to estimate the contributions of the orbital (covalent) interactions and the electrostatic attraction to the bond energy, although the question about the ionic nature of the TM-ER bond has also conversely been discussed. Several authors suggested that the TM-ER bond is largely ionic, because the population analyses showed that the transition metal carries, in most cases, a large negative charge and the atom E is highly positively charged.^{2b-d,3b,8,11} However, atomic partial charges are a very crude and sometimes misleading indicator for electrostatic interactions, because the electronic charge distribution of an atom in a molecule is not spherically symmetric. This holds true in particular for donor-acceptor bonds, which have an area of local electronic charge concentration at the donor side pointing toward the charged depleted electron acceptor atom, which leads to strong charge attraction. This is schematically shown in Figure 1b. It becomes obvious that the electrostatic attraction between $(\text{CO})_4\text{Fe}$ and ER arises from the negative local charge concentration at atom E, which has an overall positive partial charge, and the positive charge of the iron atomic nucleus, which has an area of electron depletion pointing toward the ER ligand. This has previously been proven by the topological analysis of the electron density distribution of $(\text{CO})_4\text{Fe-AlCp}^{2b}$ and $(\text{CO})_5\text{W-AlH}$.^{2c} It will be shown below that even two atoms which carry positive partial charges may electrostatically strongly attract each other because of the anisotropic electronic charge distribution.

In this work we report about an energy decomposition analysis of the TM-ER bonds of the title compounds that gives for the first time the energies that are associated with the $\text{TM} \leftarrow \text{ER} \sigma$ donation and $\text{TM} \rightarrow \text{ER} \pi$ back-donation. We also report about the strength of the ionic interactions and covalent contributions to the bond strength. Some of the results are surprising and lead to a modification of previous interpretations of the nature of the TM-ER bond. We analyzed not only the $(\text{CO})_4\text{Fe-ER}$ bonds that are trans to the strong π acceptor ligand CO, but also the bonding interactions in the homoleptic complexes $\text{Fe}(\text{EMe})_5$ and $\text{Ni}(\text{EMe})_4$. The bonding properties of the diyl ligands ER in the iron tetracarbonyl complexes are compared to the CO bonding in $\text{Fe}(\text{CO})_5$. The following questions are addressed in our work: (a) How large are the contributions of the $\text{TM} \leftarrow \text{ER} \sigma$ donation and the $\text{TM} \rightarrow \text{ER} \pi$ back-donation to the total TM-ER bonding energy? (b) How much does the strength of the $\text{TM} \rightarrow \text{ER} \pi$ back-donation alter when R changes from the good π donors Cp and $\text{N}(\text{SiMe}_2)_2$ to the poor π donors phenyl and methyl? (c) What are the relative strengths of the covalent and ionic bonding interactions that are given by the calculated attractive orbital interactions and electrostatic attraction? (d) Are there significant differences

(10) Cotton, F. A.; Feng, X. *Organometallics* **1998**, *17*, 128.

(11) (a) Boehme, C.; Frenking, G. *Chem. Eur. J.* **1999**, *5*, 2184. (b) Uddin, J.; Boehme, C.; Frenking, G. *Organometallics* **2000**, *19*, 571.

(12) Boehme, C.; Uddin, J.; Frenking, G. *Coord. Chem. Rev.* **2000**, *197*, 249.

(13) Macdonald, C. L. B.; Cowley, A. H. *J. Am. Chem. Soc.* **1999**, *121*, 12113.

(14) Davidson, E. R.; Kunze, K. L.; Machado, F. B. C.; Chakravorty, S. *J. Acc. Chem. Res.* **1993**, *26*, 628.

(15) Diefenbach, A.; Bickelhaupt, F. M.; Frenking, G. *J. Am. Chem. Soc.* **2000**, *122*, 6449.

between the TM-E bonds of the carbonyldiyl complexes $(\text{CO})_4\text{FeER}$ and the homoleptic complexes $\text{Fe}(\text{ER})_5$ and $\text{Ni}(\text{ER})_4$? How much does the strength of the $\text{TM} \rightarrow \text{ER} \pi$ back-donation change when there is no good π acceptor like CO in the trans position to ER? (e) What is the difference in the nature of the metal-ligand bonds between the ligands CO and ER?

2. Methods

The calculations were performed at the nonlocal DFT level of theory using the exchange functional of Becke¹⁶ and the correlation functional of Perdew¹⁷ (BP86). Scalar relativistic effects have been considered using the Pauli formalism.¹⁸ Uncontracted Slater-type orbitals (STOs) were used as basis functions for the SCF calculations.¹⁹ The basis sets for the metal atoms have triple- ζ quality augmented by one set of f -type polarization functions. Triple- ζ basis sets augmented by one set of d -type polarization functions have been used for the main group elements. The $(n-1)s^2$ and $(n-1)p^6$ core electrons of the main group elements and the $(1s2s2p)^{10}$ core electrons of the transition metals were treated by the frozen-core approximation.²⁰ An auxiliary set of s , p , d , f , and g STOs was used to fit the molecular densities and to represent the Coulomb and exchange potentials accurately in each SCF cycle.²¹ The calculations were carried out using the program package ADF-(2.3).²² To verify that the optimized structures are minima on the potential energy surface, we calculated the vibrational frequencies of the stationary points. The frequency calculations were carried out at BP86 with our standard basis set II³² using BP86/II-optimized geometries. This was done with the program package Gaussian 98,³³ which has analytical second derivatives.

The bonding interactions between the metal fragment $\text{Fe}(\text{CO})_4$ and the ligands ER or CO, between $\text{Fe}(\text{EMe})_4$ and EMe and between $\text{Ni}(\text{EMe})_3$ and EMe, have been analyzed using the energy decomposition scheme ETS that was developed by Ziegler and Rauk.²³ The bond dissociation energy ΔE between two fragments A and B is partitioned into several contributions that can be identified as physically meaningful entities. First, ΔE is separated into two major components ΔE_{prep} and ΔE_{int}

$$\Delta E = \Delta E_{\text{prep}} + \Delta E_{\text{int}} \quad (1)$$

ΔE_{prep} is the energy that is necessary to promote the fragments A and B from their equilibrium geometry and electronic ground state to

(16) Becke, A. D. *Phys. Rev. A* **1988**, *38*, 3098.

(17) Perdew, J. P. *Phys. Rev. B* **1986**, *33*, 8822.

(18) (a) Snijders, J. G. *Mol. Phys.* **1978**, *36*, 1789. (b) Snijders, J. G.; Ross, P. *Mol. Phys.* **1979**, *38*, 1909.

(19) Snijders, J. G.; Baerends, E. J.; Vernooijs, P. *At. Data Nucl. Data Tables* **1982**, *26*, 483.

(20) Baerends, E. J.; Ellis, D. E.; Ros, P. *Chem. Phys.* **1973**, *2*, 41.

(21) Krijn, J.; Baerends, E. J. *Fit Functions in the HFS-Method*, Internal Report (in Dutch), Vrije Universiteit Amsterdam, The Netherlands, 1984.

(22) (a) Bickelhaupt, F. M.; Baerends, E. J.; *Rev. Comput. Chem.*, in print. (b) te Velde, G.; Bickelhaupt, F. M.; Baerends, E. J.; van Gisbergen, S. J. A.; Fonseca Guerra, C.; Snijders, J. G.; Ziegler, T. *J. Comput. Chem.*, submitted.

(23) (a) Ziegler, T.; Rauk, A. *Theor. Chim. Acta* **1977**, *46*, 1. (b) Ziegler, T.; Rauk, A. *Inorg. Chem.* **1979**, *18*, 1558. (c) Ziegler, T.; Rauk, A. *Inorg. Chem.* **1979**, *18*, 1755.

(24) Examples: (a) Ziegler, T.; Tschinke, V.; Becke, A. *J. Am. Chem. Soc.* **1987**, *109*, 1351. (b) Ziegler, T.; Tschinke, V.; Ursenbach, C. *J. Am. Chem. Soc.* **1987**, *109*, 4825. (c) Li, J.; Schreckenbach, G.; Ziegler, T.; *J. Am. Chem. Soc.* **1995**, *117*, 486.

(25) Ehlers, A. W.; Baerends, E. J.; Bickelhaupt, F. M.; Radius, R. *Chem. Eur. J.* **1998**, *4*, 210.

(26) Yu, C.; Frenking, G. *J. Chem. Soc., Dalton Trans.*, in press.

(27) Wiberg, K. B. *Tetrahedron* **1968**, *24*, 1083.

(28) The radii of the valence $2s$ (boron) and $3s$ (aluminum) orbitals are 1.166 Å (B) and 1.372 Å (Al); Desclaux, J. P. *At. Data Nucl. Data Tables* **1973**, *12*, 311.

(29) Bent, H. A. *Chem. Rev.* **1961**, *61*, 275.

(30) Cremer, D.; Wu, A.; Larsson, A.; Kraka, E. *J. Mol. Model.* **2000**, *6*, 396.

(31) (a) Lupinetti, A. J.; Fau, S.; Frenking, G.; Strauss, S. H. *J. Phys. Chem. A* **1997**, *101*, 9551. (b) Goldman, A. S.; Krogh-Jespersen, K. *J. Am. Chem. Soc.* **1996**, *118*, 12159.

the geometry and electronic state that they have in the compound AB. ΔE_{int} is the instantaneous interaction energy between the two fragments in the molecule. The latter quantity shall be the focus of the present work. The interaction energy, ΔE_{int} , can be divided into three main components

$$\Delta E_{\text{int}} = \Delta E_{\text{elstat}} + \Delta E_{\text{Pauli}} + \Delta E_{\text{orb}} \quad (2)$$

ΔE_{elstat} gives the electrostatic interaction energy between the fragments that is calculated using the frozen electron density distribution of A and B in the geometry of the complex AB. The second term in eq 2, ΔE_{Pauli} , gives the repulsive interactions between the fragments that are caused by the fact that two electrons with the same spin cannot occupy the same region in space. The term comprises the four-electron destabilizing interactions between occupied orbitals. ΔE_{Pauli} is calculated by enforcing the Kohn–Sham determinant of AB, which results from superimposing fragments A and B, to obey the Pauli principle through antisymmetrization and renormalization. The stabilizing orbital interaction term ΔE_{orb} is calculated in the final step of the ETS analysis when the Kohn–Sham orbitals relax to their optimal form. The latter term can be further partitioned into contributions by the orbitals that belong to different irreducible representations of the interacting system.

Unfortunately, the first two terms, ΔE_{elstat} and ΔE_{Pauli} , are often added to a single term ΔE° , which is sometimes called the “steric energy term”.²⁴ ΔE° has nothing to do with the loosely defined steric interaction, which is often used to explain the repulsive interactions of bulky substituents. Because ΔE_{elstat} is usually attractive and ΔE_{Pauli} is repulsive, the two terms may largely cancel each other, and the focus of the discussion of the bonding interactions then rests on the orbital interaction term ΔE_{orb} . This leads to the deceptive description of the bonding only in terms of orbital interactions. The important information about the ionic/covalent character of the bond that is given by the ratio $\Delta E_{\text{elstat}}/\Delta E_{\text{orb}}$ is then lost.

3. Structural Data

The calculated geometries and TM-ER bond dissociation energies of the complexes at slightly different levels of theory have been reported in previous publications by us^{2b,3b,11,12} and by other workers^{2a,8,10,13} and, therefore, will not be discussed in detail. The most important structural data which are relevant for the discussion of the bonding situation are summarized in Table 1. The optimized geometries and calculated energies of the compounds are presented as Supporting Information.

The theoretically predicted bond dissociation energies D_e - (TM-E) and interatomic distances R(TM-ER) at BP86/TZP that are given in Table 1 are not very different from previously reported values.^{2a,b,3b,10–13} The trend of the dissociation energies of $(\text{CO})_4\text{Fe-ER}$ shows for all substituents R the following order for the elements E: B > Al > Ga > In > Tl. Our previous studies suggested that the bond energies of the gallium and indium complexes should have similar values.¹¹ The present work indicates that the Ga complexes are slightly more strongly bound than the In analogues, which is in agreement with the

(32) Frenking, G.; Antes, I.; Böhme, M.; Dapprich, S.; Ehlers, A. W.; Jonas, V.; Neuhaus, A.; Otto, M.; Stegmann, R.; Veldkamp, A.; Vyboshchikov, S. F. In *Reviews in Computational Chemistry*; Lipkowitz, K. B., Boyd, D. B., Eds; VCH: New York, 1996; Vol.8, pp 63–144.

(33) Frisch, M. J.; Trucks, G. W.; Schlegel, H. B.; Scuseria, G. E.; Robb, M. A.; Cheeseman, J. R.; Zakrzewski, V. G.; Montgomery, J. A. Jr.; Stratmann, R. E.; Burant, J. C.; Dapprich, S.; Millam, J. M.; Daniels, A. D.; Kudin, K. N.; Strain, M. C.; Farkas, O.; Tomasi, J.; Barone, V.; Cossi, M.; Cammi, R.; Mennucci, B.; Pomelli, C.; Adamo, C.; Clifford, S.; Ochterski, J.; Petersson, G. A.; Ayala, P. Y.; Cui, Q.; Morokuma, K.; Malick, D. K.; Rabuck, A. D.; Raghavachari, K.; Foresman, J. B.; Cioslowski, J.; Ortiz, J. V.; Stefanov, B. B.; Liu, G.; Liashenko, A.; Piskorz, P.; Komaromi, I.; Gomperts, R.; Martin, R. L.; Fox, D. J.; Keith, T.; Al-Laham, M. A.; Peng, C. Y.; Nanayakkara, A.; Gonzalez, C.; Challacombe, M.; Gill, P. M. W.; Johnson, B.; Chen, W.; Wong, M. W.; Andres, J. L.; Gonzalez, C.; Head-Gordon, M.; Replogle, E. S.; Pople, J. A. *Gaussian 98, Revision A.3*; Gaussian, Inc.: Pittsburgh, PA, 1998.

Table 1. Calculated Relative Energies, E_{rel} , of the Axial and Equatorial Isomers and Bond Dissociation Energies $D_{\text{c}}(\text{TM-E})$ at BP86/TZP in Kcal/Mol^a

molecule	E_{rel}	$D_{\text{c}}(\text{TM-E})$	R(TM-E)	P(TM-E)	$q(\text{TM})$	$q(\text{E})$
(CO) ₄ Fe-BCp (ax)	0.0	74.7	1.968	0.48	-0.56	0.32
(CO) ₄ Fe-BCp (eq)	4.7 ^b	^b	1.963 ^b	^b	^b	^b
(CO) ₄ Fe-ALCp (ax)	0.0	52.8	2.253	0.48	-0.58	1.18
(CO) ₄ Fe-ALCp (eq)	1.2	51.6	2.240	0.44	-0.59	1.12
(CO) ₄ Fe-GaCp (ax)	0.0	22.6	2.395	0.49	-0.51	0.96
(CO) ₄ Fe-GaCp (eq)	0.0	22.6	2.412	0.41	-0.55	0.88
(CO) ₄ Fe-InCp (ax)	0.0	19.3	2.548	0.48	-0.49	1.06
(CO) ₄ Fe-InCp (eq)	-0.2	19.5	2.658	0.40	-0.54	0.98
(CO) ₄ Fe-TlCp (ax)	0.0	13.2	2.578	0.39	-0.45	0.89
(CO) ₄ Fe-TlCp (eq)	0.7	12.5	2.600	0.32	-0.30	0.81
(CO) ₄ Fe-BN(SiH ₃) ₂ (ax)	0.0 ^b	^b	1.838 ^b	^b	^b	^b
(CO) ₄ Fe-BN(SiH ₃) ₂ (eq)	-0.4	83.9	1.828	0.65	-0.58	0.59
(CO) ₄ Fe-ALN(SiH ₃) ₂ (ax)	0.0	52.7	2.222	0.53	-0.60	1.31
(CO) ₄ Fe-ALN(SiH ₃) ₂ (eq)	-0.5	53.2	2.206	0.51	-0.63	1.23
(CO) ₄ Fe-GaN(SiH ₃) ₂ (ax)	0.0	34.6	2.310	0.53	-0.56	1.14
(CO) ₄ Fe-GaN(SiH ₃) ₂ (eq)	0.8	33.8	2.316	0.50	-0.60	1.06
(CO) ₄ Fe-InN(SiH ₃) ₂ (ax)	0.0	29.0	2.490	0.50	-0.53	1.21
(CO) ₄ Fe-InN(SiH ₃) ₂ (eq)	0.9	28.1	2.500	0.47	-0.58	1.13
(CO) ₄ Fe-TlN(SiH ₃) ₂ (ax)	0.0	20.8	2.552	0.44	-0.48	1.07
(CO) ₄ Fe-TlN(SiH ₃) ₂ (eq)	0.3	20.5	2.567	0.40	-0.54	1.00
(CO) ₄ Fe-BPh (ax)	0.0	100.2	1.803	0.76	-0.59	0.65
(CO) ₄ Fe-BPh (eq)	1.1	99.1	1.800	0.64	-0.91	0.66
(CO) ₄ Fe-AlPh (ax)	0.0	63.5	2.217	0.51	-0.60	1.27
(CO) ₄ Fe-AlPh (eq)	0.5	63.0	2.206	0.50	-0.62	1.20
(CO) ₄ Fe-GaPh (ax)	0.0	51.6	2.296	0.52	-0.56	1.12
(CO) ₄ Fe-GaPh (eq)	2.6	49.0	2.304	0.51	-0.59	1.05
(CO) ₄ Fe-InPh (ax)	0.0	45.7	2.478	0.49	-0.53	1.16
(CO) ₄ Fe-InPh (eq)	2.6	43.1	2.488	0.48	-0.56	1.08
(CO) ₄ Fe-TlPh (ax)	0.0	40.1	2.478	0.44	-0.50	1.04
(CO) ₄ Fe-TlPh (eq)	2.8	37.3	2.544	0.42	-0.59	0.98
(CO) ₄ Fe-BMe (ax)	0.0	100.1	1.800			
(CO) ₄ Fe-BMe (eq)	1.7	98.4	1.798			
(CO) ₄ Fe-AlMe (ax)	0.0	65.6	2.216			
(CO) ₄ Fe-AlMe (eq)	0.7	64.9	2.207			
(CO) ₄ Fe-GaMe (ax)	0.0	53.7	2.296			
(CO) ₄ Fe-GaMe (eq)	2.9	50.8	2.303			
(CO) ₄ Fe-InMe (ax)	0.0	48.4	2.475			
(CO) ₄ Fe-InMe (eq)	2.9	45.5	2.485			
(CO) ₄ Fe-TlMe (ax)	0.0	42.1	2.525			
(CO) ₄ Fe-TlMe (eq)	2.8	39.3	2.542			
Fe(BMe) ₅		105.6	1.782 (ax) 1.772 (eq)	0.60 (ax) 0.69 (eq)	-0.92	0.46 (ax) 0.54 (eq)
Fe(AlMe) ₅		79.2	2.182 (ax) 2.174 (eq)	0.53 (ax) 0.52 (eq)	-1.93	0.88 (ax) 1.02 (eq)
Fe(GaMe) ₅		64.2	2.252 (ax) 2.255 (eq)	0.64 (ax) 0.65 (eq)	-1.27	0.69 (ax) 0.80 (eq)
Fe(InMe) ₅		57.3	2.429 (ax) 2.434 (eq)	0.73 (ax) 0.73 (eq)	-0.94	0.63 (ax) 0.74 (eq)
Fe(TlMe) ₅		52.8	2.468 (ax) 2.474 (eq)	0.65 (ax) 0.63 (eq)	-1.11	0.62 (ax) 0.69 (eq)
Ni(BMe) ₄		92.3	1.769	0.56 ^c	0.16 ^c	0.31 ^c
Ni(AlMe) ₄		62.7	2.165	0.55	-0.42	0.71
Ni(GaMe) ₄		39.8	2.238	0.55	-0.24	0.62
Ni(InMe) ₄		41.3	2.399	0.56	-0.37	0.66
Ni(TlMe) ₄		35.8	2.447	0.56	-0.23	0.58

^a Calculated bond lengths R(TM-E) at BP86/TZP in Å. Covalent bond orders P(TM-E) and atomic partial charges q at BP86/II. The values for (CO)₄Fe-ER and Ni(EMe)₄ were taken from ref 11. ^b No energy minimum at this level of theory. ^c Calculated at B3LYP/II.

calculations of MC.¹³ Because the present calculations were carried out with larger basis sets than our previous work,¹¹ we believe that they are more reliable. The trend of the D_{e} values for the substituents R shows for all elements the order Me ~ Ph > N(SiH₃)₂ > Cp. The only exceptions are the aluminum complexes (CO)₄Fe-ALR when R is N(SiH₃)₂ and Cp, which have nearly the same bond energy.

Table 1 shows that the isomers of (CO)₄Fe-ER, where the ligand ER is in the axial position, are in most cases lower in energy than the equatorial isomers, albeit not very much. There

are four exceptions to this. The axial and equatorial forms of the complex with the ligand GaCp have nearly the same energy. The equatorial forms of (CO)₄Fe-InCp and (CO)₄Fe-ALN(SiH₃)₂ are 0.2 and 0.5 kcal/mol lower in energy than the axial forms, respectively. The calculated energy difference is too small to be significant. An intriguing case is (CO)₄Fe-BN(SiH₃)₂, which is the only compound studied by us that does not have an energy minimum structure where the ER ligand is in the axial position. Frequency calculations of the axial isomer that was optimized with C_{s} symmetry constraint showed that it is a transition state

Table 2. ETS Analysis of the Axial and Equatorial Isomers of $\text{Fe}(\text{CO})_4\text{-ECp}$ and $\text{Fe}(\text{CO})_5$ at BP86/TZP^a

	BCp		AlCp		GaCp		InCp		TlCp		CO	
	ax	eq	ax	eq	ax	eq	ax	eq	ax	eq	ax	eq
ΔE_{int}	-90.3	-79.6	-65.2	-60.3	-31.7	-25.6	-27.1	-21.7	-33.1	-25.5	-54.6	-51.4
ΔE_{Pauli}	211.6	222.5	154.3	167.9	69.8	63.6	63.6	59.9	64.1	60.8	134.8	149.9
ΔE_{elstat}	-186.0	-191.3	-112.1	-128.5	-47.1	-48.1	-40.0	-42.9	-42.7	-43.8	-98.0	-110.6
ΔE_{orb}^b	-115.9	-111.3	-107.4	-99.7	-54.4	-41.1	-50.7	-38.7	-54.2	-42.5	-91.4	-90.7
	(38.4%)	(36.8%)	(48.9%)	(43.7%)	(53.4%)	(46.0%)	(55.9%)	(47.4%)	(56.0%)	(49.2%)	(48.3%)	(45.2%)
ΔE_{σ}	-93.8	-89.5	-92.3	-85.0	-47.2	-35.3	-45.3	-36.4	-48.9	-38.3	-47.6	-43.7
ΔE_{π}^c	-22.1	-21.8	-15.1	-14.7	-7.2	-5.8	-5.4	-2.3	-5.8	-4.2	-43.8	-47.0
	(19.1%)	(19.6%)	(14.1%)	(14.7%)	(13.2%)	(14.1%)	(10.7%)	(5.9%)	(10.6%)	(9.9%)	(47.9%)	(51.8%)
ΔE_{prep}	15.0	9.6	12.5	8.8	8.7	2.7	7.3	1.7	19.5	12.4	8.1	4.7
$\Delta E (= -D_e)$	-75.3	-70.0	-52.7	-51.7	-23.0	-22.9	-19.8	-20.0	-13.6	-13.1	-46.5	-46.7

^a Energy contributions in kcal/mol. ^b The value in parentheses gives the percentage contribution to the total attractive interactions reflecting the covalent character of the bond. ^c The value in parentheses gives the percentage contribution to the total orbital interactions, ΔE_{orb} .

(one imaginary frequency). The same result has been reported before in a theoretical study using a different level of theory.^{11b} Relaxation of symmetry constraints and optimization with C_1 symmetry led to the equatorial form as the only energy-minimum structure. This is surprising, because recent theoretical calculations of the parent compound $(\text{CO})_4\text{Fe-BNH}_2$ predicted that the axial isomer is lower in energy than the equatorial isomer.²⁵ A reexamination of the relative stabilities of the axial and equatorial isomers of $(\text{CO})_4\text{Fe-BNH}_2$ showed that this result is probably not correct. Calculations at B3LYP, BP86, and CCSD(T) predict that the equatorial isomer is 2–3 kcal/mol more stable than the axial form.²⁶

A comparison of the calculated Fe-EMe bond lengths and bond energies of the carbonyl complexes $(\text{CO})_4\text{Fe-EMe}$ with the values that are predicted for the homoleptic molecules $\text{Fe}(\text{EMe})_5$, which have not been calculated before, shows that the latter compounds have shorter and clearly stronger Fe-EMe bonds than do the former species. This is an important piece of information for the experiment, because homoleptic complexes with group-13 diyl ligands could only be synthesized for Ni, Pd, and Pt³ but not for the group-8 elements Fe, Ru, and Os. The calculations suggest that such complexes should be quite stable thermodynamically, because the $(\text{EMe})_4\text{Fe-EMe}$ bond energies are even higher than the D_e values of the $(\text{EMe})_3\text{Ni-EMe}$ bonds (Table 1).

Table 1 also shows the atomic partial charges of the atoms TM and E and the Wiberg²⁷ bond orders $P(\text{TM-E})$ in the complexes. Note that the iron atom in $\text{Fe}(\text{EMe})_5$ carries a large negative charge, but the nickel atom in $\text{Ni}(\text{EMe})_4$ is positively charged. The charge distribution seems to indicate a significantly different bonding situation in the two sets of homoleptic complexes. It will be shown below that the calculated partial charges and the bond orders are not very useful when the energy contributions of the chemical bond are estimated.

4. Analysis of the TM-ER Bonding Situation

4.1 Complexes $(\text{CO})_4\text{Fe-ECp}$. Table 2 gives the calculated values of the bond energy partitioning for the axial and equatorial isomers of $(\text{CO})_4\text{Fe-ECp}$. To compare the bonding situation of the ECp ligand with CO, we also show the calculated energy terms of $\text{Fe}(\text{CO})_5$. Figure 2 shows a diagram of the absolute values of the repulsive term ΔE_{Pauli} , the attractive electrostatic term ΔE_{elstat} , and orbital interaction term ΔE_{orb} . It also shows the contributions of the π orbital interactions ΔE_{π} to ΔE_{orb} .

The breakdown of the energy components of ΔE_{int} into the repulsive term ΔE_{Pauli} and the attractive terms ΔE_{elstat} and ΔE_{orb} shows that ΔE_{Pauli} always has the largest absolute value (Table

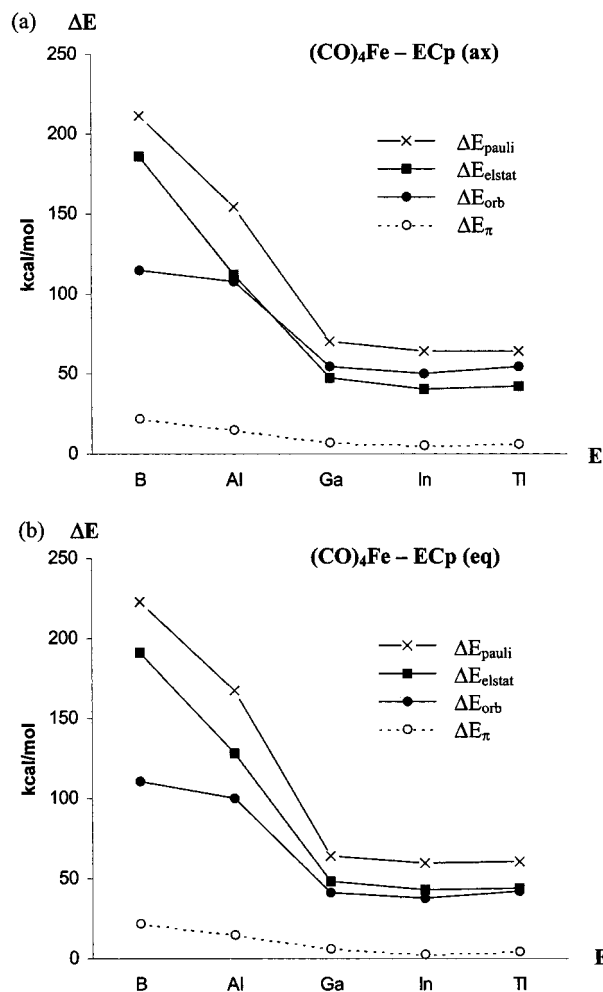


Figure 2. Absolute values of the energy contributions of the Pauli repulsion ΔE_{Pauli} , electrostatic interactions ΔE_{elstat} , total orbital interactions ΔE_{orb} , and π orbital interactions ΔE_{π} to the Fe-E bonding interactions in $(\text{CO})_4\text{Fe-ECp}$. (a) Axial isomers, (b) equatorial isomers.

2). Figure 2 shows that the trends of ΔE_{elstat} and ΔE_{Pauli} from boron to thallium are roughly parallel to each other. The values of both terms change very little for the heavier elements Ga–Tl, but they rise sharply for the lighter elements Al and, particularly, B. The attractive orbital interaction term ΔE_{orb} exhibits a trend similar to ΔE_{elstat} and ΔE_{Pauli} for the elements Al–Tl. However, the ΔE_{orb} value of the boron complex is only slightly higher than for aluminum, although the other two terms sharply increase. The somewhat unexpected conclusion is that the boron complex $(\text{CO})_4\text{Fe-BCp}$ has the largest percentage of

Table 3. ETS Analysis of the Axial and Equatorial Isomers of $\text{Fe}(\text{CO})_4\text{-EN}(\text{SiH}_3)_2$ at BP86/TZP^a

	BN(SiH ₃) ₂		AlN(SiH ₃) ₂		GaN(SiH ₃) ₂		InN(SiH ₃) ₂		TlN(SiH ₃) ₂	
	ax ^b	eq	ax	eq	ax	eq	ax	eq	ax	eq
ΔE_{int}	-92.9	-91.9	-60.5	-57.9	-42.9	-38.0	-36.5	-30.8	-28.6	-23.4
ΔE_{Pauli}	229.9	261.3	143.5	158.1	95.2	95.1	81.0	80.5	63.3	61.7
ΔE_{elstat}	-187.6	-211.5	-99.3	-118.1	-67.7	-73.4	-55.4	-60.1	-40.9	-44.3
ΔE_{orb}^c	-135.2 (41.9%)	-141.7 (40.1%)	-104.7 (51.3%)	-97.9 (45.3%)	-70.4 (50.9%)	-59.7 (44.9%)	-62.1 (52.9%)	-51.2 (46.0%)	-51.0 (55.5%)	-40.7 (47.9%)
ΔE_{σ}	-94.0	-94.0	-85.6	-76.0	-57.6	-45.7	-53.1	-41.3	-43.7	-32.9
ΔE_{π}^d	-41.2 (30.5%)	-47.7 (33.7%)	-19.1 (18.2%)	-21.9 (22.4%)	-12.8 (18.2%)	-14.0 (23.5%)	-9.0 (14.5%)	-9.9 (19.3%)	-7.3 (14.3%)	-7.8 (19.2%)
ΔE_{prep}	9.3	8.5	8.9	6.4	8.4	4.4	7.6	3.3	7.9	3.0
$\Delta E (= -D_{\text{e}})$	-83.6	-83.4	-51.6	-51.5	-34.5	-33.6	-28.9	-27.5	-20.7	-20.4

^a Energy contributions in kcal/mol ^b Not an energy minimum; see text. ^c The value in parentheses gives the percentage contribution to the total attractive interactions reflecting the covalent character of the bond. ^d The value in parentheses gives the percentage contribution to the total orbital interactions, ΔE_{orb} .

ionic character and thus, the lowest percentage covalent character (38.4% in the axial isomer; Table 2) among the compounds $(\text{CO})_4\text{Fe-ECp}$, although the ΔE_{orb} term of $(\text{CO})_4\text{-BCp}$ has the largest absolute value. The electrostatic term contributes 61.6% to the total attractive interactions in axial $(\text{CO})_4\text{Fe-BCp}$, although in the other ECp complexes, the covalent contributions (48.9–56.0% in the axial isomers) and the ionic contributions have a similar strength. The complex $(\text{CO})_4\text{Fe-TlCp}$ has the highest percentage covalent character.

The similar trends of ΔE_{orb} and ΔE_{elstat} of the ECp complexes (which is also found for the other ER complexes; see below) for the heavier elements E and the comparatively small ΔE_{orb} value of the boron compound can be explained by the symmetry of the interacting orbitals. Table 2 and Figure 2 show that the dominant contributions to ΔE_{orb} come from σ interactions. Figure 1a shows that the σ donor orbital of E at first overlaps in a bonding fashion with the loop of the d_{z^2} acceptor orbital of TM, which has the same sign. However, at shorter distances, there is an overlap with the tubular-shaped loop of the d_{z^2} orbital, which has an opposite sign, leading to antibonding orbital interactions with the σ donor orbital. The electrostatic interactions (Figure 1b) do not depend on the sign of the occupied orbitals that contribute to the electrostatic term. The sign effect becomes important when the donor and acceptor atoms come closer to each other. Boron has clearly the shortest equilibrium distance of the TM-E bonds (Table 1). The radii of the boron valence orbitals are smaller than those of the aluminum orbitals, but the difference of the radii is less than the difference in the Fe-ECp bond lengths.²⁸ The overlap of the σ donor and acceptor orbitals of boron and iron are only slightly larger (0.426) than those of the aluminum complex (0.412, which explains why the ΔE_{orb} term of boron is not much higher than that of the aluminum complex. Note that this behavior is already found for the equatorial isomer of $(\text{CO})_4\text{Fe-AlCp}$. Figure 2 shows that the ΔE_{orb} value of the latter is clearly smaller than the ΔE_{elstat} value, although in the axial isomer, the two terms have nearly the same strength. The Fe-AlCp distance of the equatorial form (2.240 Å) is shorter than that in the axial form (2.253 Å). However, we want to point out that the size of ΔE_{orb} and ΔE_{elstat} is not simply a function of the interatomic distance. The latter depends on the topology of the charge distribution, and the former depends on the energy values and the spacial distribution of the interacting orbitals.

Table 2 also gives the breakdown of the ΔE_{orb} term into contributions of $\text{Fe} \leftarrow \text{ECp} \sigma$ donation and $\text{Fe} \rightarrow \text{ECp} \pi$ back-donation. It becomes obvious that the latter term is, in all complexes, much smaller than the σ donation. This is also graphically shown in Figure 2. The largest π contribution is

found in the equatorial isomer of the boron complex where the $\text{Fe} \rightarrow \text{B} \pi$ back-donation has 19.6% of the ΔE_{orb} term (Table 2). It follows that the ECp ligand for all elements E dominantly behaves as a σ donor. This is clearly different from the ligand CO in $\text{Fe}(\text{CO})_5$. Table 2 shows that the energy contributions of the $\text{Fe} \leftarrow \text{CO} \sigma$ donation and $\text{Fe} \rightarrow \text{CO} \pi$ back-donation in the pentacarbonyl have a comparable strength. The bonding interactions ΔE_{int} and bond dissociation energy ΔE of the axial and equatorial Fe-CO bonds are much smaller than the values of the Fe-BCp bonds and even smaller than the Fe-AlCp bonds. The ΔE_{elstat} value of the Fe-CO bond is only slightly higher than the ΔE_{orb} value, which indicates that the ionic and covalent contribution have the same magnitude. The Fe-BCp bond, which is stronger when compared to Fe-CO, comes mainly from the large ionic contribution in the former bond.

We want to point out that for all complexes, $(\text{CO})_4\text{TM-ECp}$ holds that $\Delta E_{\text{elstat(ax)}} < \Delta E_{\text{elstat(eq)}}$ and $\Delta E_{\text{orb(ax)}} > \Delta E_{\text{orb(eq)}}$. It will be shown below that the axial isomers of all diyl complexes $(\text{CO})_4\text{Fe-ER}$ have a higher percentage of orbital interactions and a lower degree of ionic interactions than do the equatorial isomers. We also want to point out that the atomic partial charges shown in Table 1, which suggest that there are strong charge attractions between Fe and E, give the right answer for the wrong reason. The charge attraction arises mainly from the attraction of the negative electronic charge of the σ donor electron pair of E with the positively charged nucleus of Fe (Figure 1b) and not between positively charged E and negatively charged Fe. The calculated atomic partial charges are also misleading for an estimate of the trend of the electrostatic forces. The partial charge of boron in $(\text{CO})_4\text{Fe-BCp}$ (+0.32) is much smaller than the charges of the heavier atoms E (+0.81 to +1.18, Table 1), but the electrostatic attraction in the Fe-BCp bond is much higher than in the other Fe-ECp bonds (Table 2).

4.2 Complexes $(\text{CO})_4\text{Fe-EN}(\text{SiH}_3)_2$. Table 3 gives the results of the ETS analysis of the complexes $(\text{CO})_4\text{Fe-EN}(\text{SiH}_3)_2$. The trend of the different energy terms is displayed in Figure 3. Figure 3 shows that the trends of the energy terms ΔE_{Pauli} , ΔE_{elstat} , and ΔE_{orb} are quite similar to the curves which are found for the ECp complexes (Figure 2). The boron complex $(\text{CO})_4\text{Fe-BN}(\text{SiH}_3)_2$ has, again, a higher ionic character than the other $\text{EN}(\text{SiH}_3)_2$ complexes, which have nearly equal contributions by ΔE_{elstat} and ΔE_{orb} .

The curve of ΔE_{orb} increases from $(\text{CO})_4\text{Fe-AlN}(\text{SiH}_3)_2$ to $(\text{CO})_4\text{Fe-BN}(\text{SiH}_3)_2$ more sharply than it does from $(\text{CO})_4\text{Fe-AlCp}$ to $(\text{CO})_4\text{Fe-BCp}$ (Figure 2), although the Fe-BN(SiH₃)₂ equilibrium distances are clearly shorter than the Fe-BCp bond lengths (Table 1). This finding seems to disprove our argument that the σ donor orbital of boron encounters destabilizing

Table 4. ETS Analysis of the Axial and Equatorial Isomers of $\text{Fe}(\text{CO})_4\text{-EPh}$ at BP86/TZP^a

	BPh		AlPh		GaPh		InPh		TlPh	
	ax	eq	ax	eq	ax	eq	ax	eq	ax	eq
ΔE_{int}	-110.3	-109.8	-73.2	-71.1	-61.0	-55.5	-48.8	-48.7	-49.4	-42.9
ΔE_{Pauli}	276.6	319.2	173.8	192.3	129.5	130.0	112.3	112.2	98.7	96.4
ΔE_{elstat}	-230.4	-258.8	-127.3	-147.6	-102.3	-107.5	-87.0	-91.7	-79.3	-81.3
ΔE_{orb}^c	-156.5	-170.2	-119.7	-115.8	-88.2	-76.0	-74.1	-69.2	-68.8	-58.0
	(40.4%)	(39.7%)	(48.5%)	(44.0%)	(46.3%)	(42.0%)	(46.0%)	(43.0%)	(46.5%)	(41.4%)
ΔE_{σ}	-104.3	-110.3	-98.2	-91.6	-73.0	-61.7	-63.4	-57.7	-59.8	-48.6
ΔE_{π}^d	-52.2	-59.9	-21.5	-24.2	-15.2	-16.3	-10.7	-11.5	-9.0	-9.4
	(33.4%)	(35.2%)	(18.0%)	(20.9%)	(17.2%)	(20.9%)	(14.4%)	(16.6%)	(13.1%)	(16.2%)
$\Delta E_{\pi(b1)}^b$		-39.3		-15.6		-11.4		-8.2		-6.7
$\Delta E_{\pi(b2)}^b$		-20.7		-8.6		-4.9		-3.3		-2.7
ΔE_{prep}	10.1	10.8	9.4	8.2	8.7	6.1	8.1	5.2	8.6	4.9
$\Delta E (= -D_c)$	-100.2	-99.0	-63.8	-62.9	-52.3	-49.4	-40.7	-43.5	-40.8	-38.0

^a Energy contributions in kcal/mol. ^b π (b1) orbital is in the Ph plane and π (b2) orbital is perpendicular to the Ph plane. ^c The value in parentheses gives the percentage contribution to the total attractive interactions reflecting the covalent character of the bond. ^d The value in parentheses gives the percentage contribution to the total orbital interactions, ΔE_{orb} .

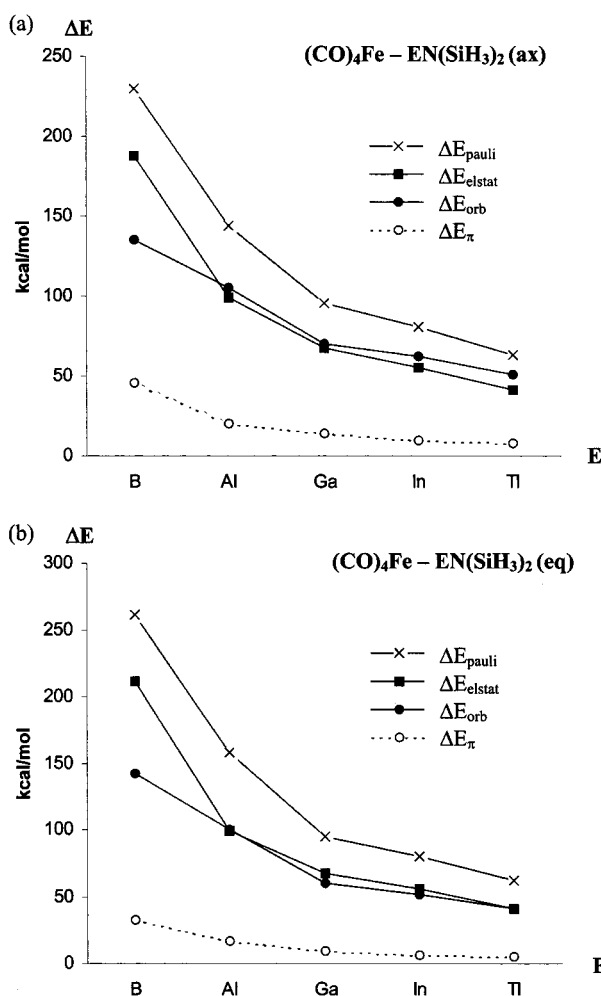


Figure 3. Absolute values of the energy contributions of the Pauli repulsion ΔE_{Pauli} , electrostatic interactions ΔE_{elstat} , total orbital interactions ΔE_{orb} , and π orbital interactions ΔE_{π} to the Fe-E bonding interactions in $(\text{CO})_4\text{Fe-EN}(\text{SiH}_3)_2$. (a) Axial isomers, (b) equatorial isomers.

interactions at shorter distances because of antibonding overlapping with the tubular-shaped loop of the d_{z^2} acceptor orbital. However, the higher value of the ΔE_{orb} term in $(\text{CO})_4\text{Fe-BN}(\text{SiH}_3)_2$ when compared to $(\text{CO})_4\text{Fe-AlN}(\text{SiH}_3)_2$ is largely caused by the $\text{Fe} \rightarrow \text{B} \pi$ back-donation (Table 3). The increase in the ΔE_{orb} term of the boron complex is mainly due to the π back-donation, which is much higher than in the aluminum complex.

The calculated π back-donation in $(\text{CO})_4\text{Fe-BN}(\text{SiH}_3)_2$ is half as strong as σ donation. Tables 2 and 3 show that the $\text{Fe} \rightarrow \text{EN}(\text{SiH}_3)_2 \pi$ back-donation is for all elements E stronger than the $\text{Fe} \rightarrow \text{ECp} \pi$ back-donation. The same order has been found in the analysis of the electronic structure of the complexes.^{11b} The substituent $\text{N}(\text{SiH}_3)_2$ is only a two-electron π donor in $\text{EN}(\text{SiH}_3)_2$, but Cp is a four-electron π donor in ECp. The calculated values for the ΔE_{π} interactions in the complexes $(\text{CO})_4\text{Fe-ECp}$ and $(\text{CO})_4\text{Fe-EN}(\text{SiH}_3)_2$ show that the $\text{Fe} \rightarrow \text{ER} \pi$ back-donation can to some extent be modulated by the substituent R. However, the bonding contribution of the $\text{Fe} \leftarrow \text{ECp} \sigma$ donation remains the dominant part of the total orbital interactions ΔE_{orb} . The largest π back-donation (33.7%) is calculated for $(\text{CO})_4\text{Fe-BN}(\text{SiH}_3)_2$ (Table 3).

4.3 Complexes $(\text{CO})_4\text{Fe-EPh}$. Table 4 gives the results of the ETS analysis of the complexes $(\text{CO})_4\text{Fe-EPh}$. The trend of the different energy terms is shown in Figure 4.

The ΔE_{int} values of the ligand EPh with the poor σ donor substituent phenyl are clearly higher than the bonding energies of the ligands ECp and $\text{EN}(\text{SiH}_3)_2$ (Tables 2–4). Inspection of the different energy terms shows, however, that the $\text{Fe} \rightarrow \text{EPh} \pi$ back-donation contributes little to the enhanced binding interactions. The ΔE_{π} values of the complexes $(\text{CO})_4\text{Fe-EPh}$ are only slightly higher than the values of the ECp and $\text{EN}(\text{SiH}_3)_2$ complexes. It follows that the substituent R has only a limited influence on the strength of the $\text{Fe} \rightarrow \text{ER} \pi$ back-donation if a strong π acceptor ligand competes with the ER ligand. Table 4 shows that the higher ΔE_{int} values of the more stable axial EPh complexes are caused by stronger $\text{Fe} \leftarrow \text{EPh} \sigma$ donation and particularly by higher Coulombic attraction. This becomes obvious by the curves of the energy terms, which are shown in Figure 4. The ΔE_{elstat} values are always higher than the ΔE_{orb} values. This holds in particular for the equatorial isomers, which have a substantially higher ionic character than the axial forms. The boron complexes again have the highest percentage of ionic character.

The ETS analysis of the equatorial isomers of the $(\text{CO})_4\text{Fe-EPh}$ complexes reveals the different contributions of the $\text{Fe} \rightarrow \text{EPh} \pi$ back-donation with respect to the π orbitals which are in-plane and out-of-plane with the phenyl ring (Figure 5). Table 4 shows that the in-plane contribution is always about twice as strong as the out-of-plane contribution. This is reasonable, because the out-of-plane $p(\pi)$ AO of atom E is stabilized by π conjugation from the phenyl ring, whereas the in-plane $p(\pi)$ AO is empty. The absolute contribution of the $\text{Fe} \rightarrow \text{BPh} \pi$ back-donation has a value similar to the $\text{Fe} \rightarrow \text{CO} \pi$ back-

Table 5. ETS <tbltlt;2>Analysis of the Axial and Equatorial Isomers of $\text{Fe}(\text{CO})_4\text{-ECH}_3$ at BP86/TZP^a

	BCH ₃		AlCH ₃		GaCH ₃		InCH ₃		TlCH ₃	
	ax	eq	ax	eq	ax	eq	ax	eq	ax	eq
ΔE_{int}	-110.0	-108.8	-74.4	-72.9	-62.0	-56.7	-56.3	-50.8	-51.2	-51.6
ΔE_{Pauli}	274.2	322.4	178.9	201.6	133.4	138.7	119.1	120.6	104.8	103.6
ΔE_{elstat}	-228.2	-258.8	-131.5	-153.9	-106.1	-114.0	-93.7	-99.0	-83.2	-85.7
ΔE_{orb}^b	-156.0	-172.4	-121.8	-120.6	-89.3	-81.4	-81.7	-72.4	-72.8	-69.5
	(40.6%)	(40.0%)	(48.1%)	(43.9%)	(45.7%)	(41.7%)	(46.6%)	(42.2%)	(46.6%)	(44.8%)
ΔE_{σ}	-105.5	-127.8	-101.0	-101.9	-75.0	-71.1	-71.4	-65.3	-64.3	-75.1
ΔE_{π}^c	-50.5	-44.6	-20.8	-18.7	-14.3	-10.3	-10.3	-7.1	-8.5	5.6
	(32.4%)	(25.9%)	(17.1%)	(15.5%)	(16.0%)	(12.7%)	(12.6%)	(9.8%)	(11.7%)	(6.9%)
ΔE_{prep}	10.0	10.7	9.0	8.3	8.2	5.9	7.9	5.3	5.4	5.2
$\Delta E (= -D_c)$	-100.0	-98.1	-65.4	-64.6	-53.8	-50.8	-48.4	-45.5	-45.8	-46.4

^a Energy contributions in kcal/mol ^b The value in parentheses gives the percentage contribution to the total attractive interactions reflecting the covalent character of the bond. ^c The value in parentheses gives the percentage contribution to the total orbital interactions ΔE_{orb} .

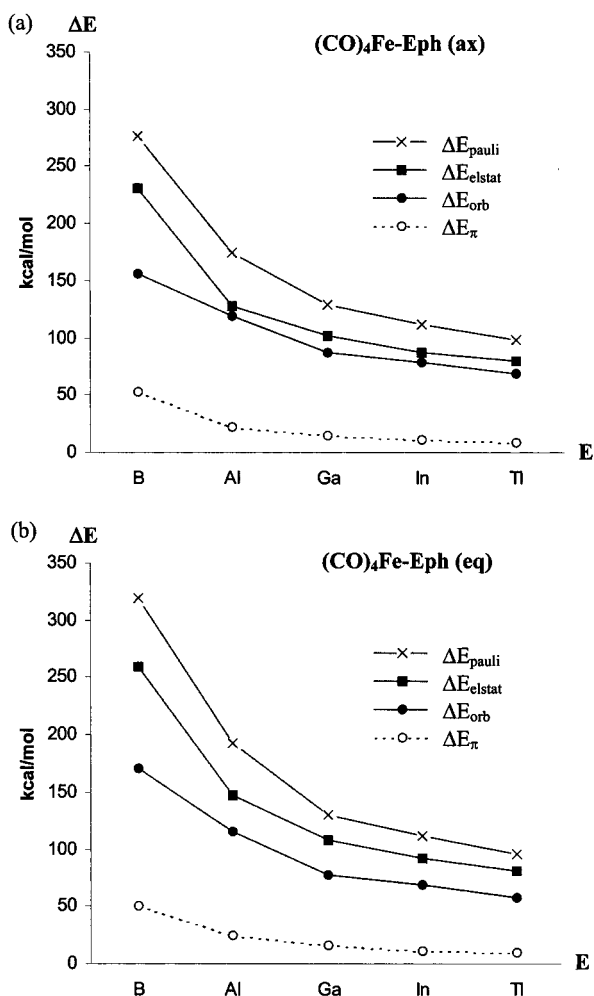


Figure 4. Absolute values of the energy contributions of the Pauli repulsion ΔE_{Pauli} , electrostatic interactions ΔE_{elstat} , total orbital interactions ΔE_{orb} , and π orbital interactions ΔE_{π} to the Fe-E bonding interactions in $(\text{CO})_4\text{Fe-EPh}$. (a) Axial isomers, (b) equatorial isomers.

donation in $\text{Fe}(\text{CO})_5$ (Table 2), but the ratio of the energy contribution of donation and back-donation still makes BPh a stronger donor than acceptor, whereas CO has similar donor and acceptor strengths.

4.4 Complexes $(\text{CO})_4\text{Fe-EMe}$. Table 5 gives the results of the ETS analysis of the complexes $(\text{CO})_4\text{Fe-EMe}$. The trend of the different energy terms is shown in Figure 6.

A comparison of the ETS results of the EMe complexes with the bonding analysis of the EPh complexes (Table 4 and Figure 4) shows that the values of the energy terms are nearly the same.

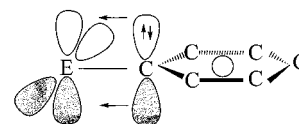


Figure 5. Schematic representation of the π bonding interactions in TM-EPh.

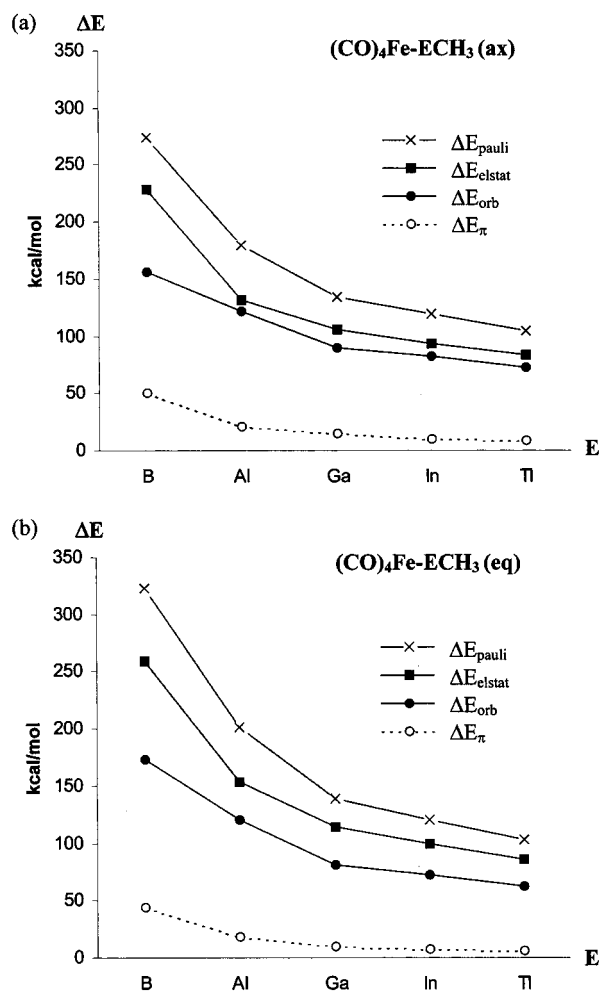


Figure 6. Absolute values of the energy contributions of the Pauli repulsion ΔE_{Pauli} , electrostatic interactions ΔE_{elstat} , total orbital interactions ΔE_{orb} , and π orbital interactions ΔE_{π} to the Fe-E bonding interactions in $(\text{CO})_4\text{Fe-EMe}$. (a) Axial isomers, (b) equatorial isomers.

An interesting difference between the two sets of compounds concerns the σ and π contributions to the ΔE_{orb} term. The strength of the σ and π orbital interactions in the axial isomers

Table 6. ETS Analysis of the Equatorial Fe-E Bonds of the Complexes Fe(ECH₃)₅ at BP86/TZP^a

	BCH ₃	AlCH ₃	GaCH ₃	InCH ₃	TlCH ₃
ΔE_{int}	-119.2	-87.0	-67.0	-59.5	-54.1
ΔE_{Pauli}	247.8	140.2	120.8	113.9	113.0
ΔE_{elstat}	-228.4	-135.4	-115.2	-107.8	-103.8
ΔE_{orb}^b	-138.6	-91.8	-72.6	-65.6	-63.3
	(37.8%)	(40.4%)	(38.7%)	(37.8%)	(37.9%)
ΔE_{σ}	-74.6	-55.0	-45.5	-41.7	-42.9
ΔE_{π}^c	-64.0	-36.8	-27.1	-23.9	-20.4
	(46.2%)	(40.1%)	(37.3%)	(36.4%)	(32.2%)
ΔE_{prep}	13.6	7.8	2.9	2.1	1.1
$\Delta E (= -D_c)$	-105.6	-79.2	-64.1	-57.4	-53.1

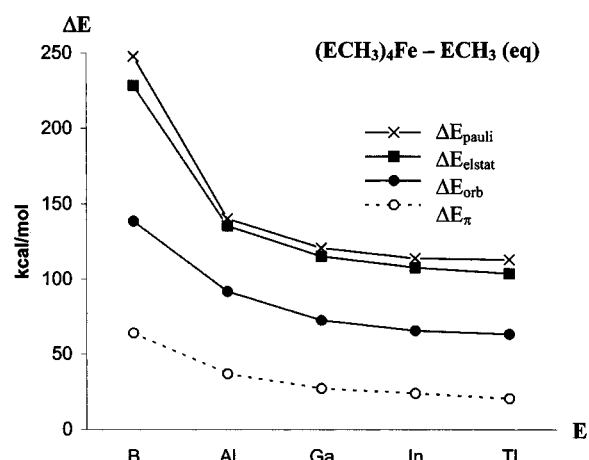
^a Energy contributions in kcal/mol. ^b The value in parentheses gives the percentage contribution to the total attractive interactions reflecting the covalent character of the bond. ^c The value in parentheses gives the percentage contribution to the total orbital interactions, ΔE_{orb} .

is nearly the same. The Fe \rightarrow EPh π back-donation is stronger than the Fe \rightarrow EMe π back-donation in the equatorial isomers, but the latter compounds have stronger σ interactions than the equatorial EPh compounds, which leads to similar ΔE_{orb} values. It follows that the Fe-ER bonding situation of group-13 diyl complexes with alkyl substituents R should be quite similar to complexes with aryl substituents. This is an important prediction for experimental studies. There is only one group-13 diyl complex with an aryl substituent that has been synthesized so far by Robinson, that is, the gallium complex (CO)₄Fe-GaAr* (Ar* = 2,6-(2,4,6-triisopropylphenyl)-phenyl).⁶ The calculated results predict that analogous diyl complexes with bulky alkyl substituents might also become isolable.

4.5 Complexes Fe(EMe)₅. The energy-partitioning analysis of the complexes (CO)₄Fe-ER has shown that the Fe \rightarrow ER π back-donation is significantly weaker than the Fe \leftarrow ER σ donation even when R is phenyl and methyl. The ligand ER competes in the carbonyl complexes with strong Fe \rightarrow CO π back-donation. To address the question of whether the Fe \rightarrow ER π back-donation becomes more important when there are no other π acceptor ligands in the complex, we analyzed the bonding situation in the homoleptic complexes Fe(EMe)₅. We present only the results of the equatorial Fe-EMe bonds because some calculations of the axial bonds failed because of convergence problems.

Table 6 shows the results of the ETS analysis of the complexes Fe(EMe)₅. The trend of the different energy terms is shown in Figure 7.

A comparison of the ETS results that were obtained for the complexes (CO)₄Fe-EMe (Table 5) and Fe(EMe)₅ (Table 6) shows significant differences. The Fe-EMe bonds of the homoleptic complexes Fe(EMe)₅ have a higher degree of ionic character than do the (CO)₄Fe-EMe bonds. This holds particularly for the heavier group-13 elements Al-Tl. The difference becomes obvious by a comparison of the trend of the energy terms that are displayed in Figures 6 and 7. Table 6 shows that the electrostatic term is about 1.5 times larger than the orbital interaction term. The Fe-EMe bonds of the homoleptic complexes are shorter than those of the carbonyl complexes, which leads to a higher ionic character. Please note that the covalent character of the Fe-EMe bonds in the homoleptic complexes Fe(EMe)₅ is nearly the same for all elements E, although the Fe-BR bonds in (CO)₄FeBR have a clearly higher ionic character than do the heavier atoms. This becomes obvious by the ratio $\Delta E_{\text{orb}}/\Delta E_{\text{elstat}}$. Table 6 shows that ΔE_{orb} contributes between 37.8% (E = B, In) and 40.4% (E = Al) to the total attractive interactions in the Fe-EMe bonds. We want to point out that

**Figure 7.** Absolute values of the energy contributions of the Pauli repulsion ΔE_{Pauli} , electrostatic interactions ΔE_{elstat} , total orbital interactions ΔE_{orb} , and π orbital interactions ΔE_{π} to the Fe-E (equatorial) bonding interactions in Fe(EMe)₅.

the Fe-BMe and Fe-AlMe bonds of the homoleptic complexes have larger interaction energies and bond dissociation energies than the tetracarbonyl complexes, although the attractive terms ΔE_{orb} and ΔE_{elstat} are higher in the latter than in the former (Tables 5 and 6). The stronger and shorter bonds in Fe(BMe)₅ and Fe(AlMe)₅ come from the lower ΔE_{Pauli} values. This is an important result because shorter and stronger bonds are often explained by stronger bonding interactions.

Another difference between the carbonyl diyl complexes and the homoleptic complexes concerns the relative contributions of the σ and π orbital contributions to the ΔE_{orb} term. The entries in Tables 5 and 6 and the curves displayed in Figures 6 and 7 indicate that the Fe \rightarrow EMe π back-donation makes a significant contribution to the orbital interactions. This holds particularly for Fe(BMe)₅, where the Fe \rightarrow EMe π back-donation is nearly as strong as the Fe \leftarrow BMe σ donation. Fe \rightarrow EMe π back-donation is always \geq one-half of Fe \rightarrow ER σ donation, even in the heavier Fe(EMe)₅ analogues. In addition, the absolute values of ΔE_{π} in Fe(EMe)₅ are clearly higher than in (CO)₄Fe-EMe. The results clearly prove that the ligands ER may become strong π acceptors if other strong π acceptor ligands are absent. A comparison³⁵ of the ETS results of Fe(BMe)₅ with those of Fe-(CO)₅ (Table 2) shows that BMe is nearly as strong a π acceptor (46.2% of ΔE_{orb}) as CO (51.8% of ΔE_{orb}) is in homoleptic complexes. The absolute values of ΔE_{π} in Fe(BMe)₅ are even higher than in Fe(CO)₅. The main difference between the Fe-BMe and Fe-CO bonds is that the former has a clearly higher degree of electrostatic interactions.

4.6 Complexes Ni(EMe)₄. The energy partitioning analysis of the complexes Fe(EMe)₅ has shown that the Fe \rightarrow ER π back-donation can significantly contribute to the ΔE_{orb} term but that the Fe-EMe bonds in the homoleptic complexes have a much larger ionic contribution than they do in (CO)₄Fe-EMe. Homoleptic complexes of iron with group-13 diyl ligands could not become synthesized so far, despite experimental efforts,³⁴ but homoleptic complexes of nickel Ni(ER)₄ for when E is Ga and In with bulky alkyl groups R are known.³ The difficulty for synthesizing homoleptic iron complexes cannot be due to the weakness of the bonds, because the calculated bond energies

(34) Uhl, W.; personal communication.

(35) It may be argued that a comparison of CO and BR ligands should be made between CO_{trans} and BR in (CO)₄Fe-BR. We prefer to compare the ligand BR in (CO)₄Fe-BR to CO in Fe(CO)₅, because the two ligands have the same surroundings.

Table 7. ETS Analysis of the Complexes Ni(ECH₃)₄ at BP86/TZP^a

	BCH ₃	AlCH ₃	GaCH ₃	InCH ₃	TlCH ₃
ΔE_{int}	-95.7	-64.7	-50.1	-43.9	-40.8
ΔE_{Pauli}	236.8	131.5	113.6	105.8	103.7
ΔE_{elstat}	-215.9	-123.2	-107.3	-99.8	-96.1
ΔE_{orb}^b	-116.6	-73.0	-56.4	-49.9	-48.4
	(35.1%)	(37.2%)	(34.5%)	(33.3%)	(33.6%)
ΔE_{σ}	-60.0	-45.3	-33.9	-30.5	-31.2
ΔE_{π}^c	-56.6	-27.7	-22.5	-19.4	-17.2
	(48.5%)	(37.9%)	(39.9%)	(38.9%)	(35.5%)
ΔE_{prep}	3.4	3.1	3.5	3.2	5.1
$\Delta E (= -D_e)$	-92.3	-61.6	-46.6	-40.7	-35.7

^a Energy Contributions in kcal/mol. ^b The value in parentheses gives the percentage contribution to the total attractive interactions reflecting the covalent character of the bond. ^c The value in parentheses gives the percentage contribution to the total orbital interactions, ΔE_{orb} .

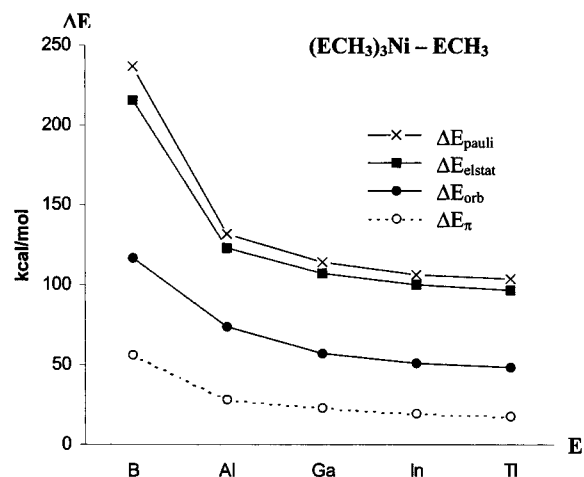


Figure 8. Absolute values of the energy contributions of the Pauli repulsion ΔE_{Pauli} , electrostatic interactions ΔE_{elstat} , total orbital interactions ΔE_{orb} , and π orbital interactions ΔE_{π} to the Ni-E bonding interactions in Ni(EMe)₄.

of Fe(EMe)₅ are higher than those of Ni(EMe)₄. The calculated partial charges (Table 1) suggest that the nature of the TM-EMe bonds in the two sets of homoleptic compounds may perhaps be different. We, therefore, analyzed the bonding situation in the complexes Ni(EMe)₄ and compared the results to the data for Fe(EMe)₅. Previous investigations of the electronic structure of TM(EMe)₄ when TM is Ni, Pd, and Pt have shown that the TM → EMe π charge donation is rather high.^{3b,11b}

Table 7 shows the results of the ETS analysis of the complexes Ni(EMe)₄. The trend of the different energy terms is shown in Figure 8.

The data given in Table 7 show that the nature of the Ni-EMe bonds is not very different from the Fe-EMe bonds in Fe(EMe)₅ (Table 6). The Ni-EMe bonds are slightly less covalent than the Fe-EMe bonds. Ni → EMe π back-donation contributes slightly more to the total ΔE_{orb} values in Ni(EMe)₄ than Fe → EMe π back-donation does in Fe(EMe)₅. Thus, the bonding situation in Ni(EMe)₄ is not so different from Fe(EMe)₅ as the calculated partial charges for Ni and Fe (Table 1) suggest. The results demonstrate clearly that the atomic partial charges cannot be taken as a measure of the electrostatic interactions between the atoms. Table 1 shows that the boron atoms in Ni(BMe)₄ carry a positive charge of 0.16 *e* and that the nickel atom also has a positive charge of 0.56 *e*. A naive conclusion would be that the electrostatic interactions between nickel and

boron are repulsive. Table 7 shows that there are strong Coulombic attractions between Ni and B, with $E_{\text{elstat}} = -215.9$ kcal/mol. The strong charge attraction is caused by the anisotropic charge distribution of the electrons. The positively charged boron atom has a lone electron pair that is directed toward the metal atom (Figure 1b). The same situation is found in Fe(BMe)₅. This is the reason the electrostatic attraction in the latter compound ($E_{\text{elstat}} = -228.4$ kcal/mol, Table 6) is nearly the same as in Ni(BMe)₄.

5. Discussion

The results of the energy partitioning analysis presented in our work lead to a consistent picture of the nature of the TM-ER bond. The group-13 diyl ligands ER are clearly stronger σ donors than π acceptors in the tetracarbonyldiyl complexes (CO)₄Fe-ER, even when the substituent R is a poor π donor. This is in agreement with previous investigations of the charge distribution by several authors.^{10–13} The novel finding is that the strength of the TM → ER π back-donation becomes a significant part of the orbital interactions in homoleptic diyl complexes. The ligand BMe is nearly as strong a π acceptor in Fe(BMe)₅ as CO is in Fe(CO)₅. Another important result is the finding that, in all of the complexes that were investigated, the electrostatic interactions contributed between 44% (in (CO)₄Fe-TlCp) and 66% (in Ni(TlMe)₄) to the total attractive interactions between the metal and the ER ligand. The ionic character in the TM-E bonds of the homoleptic complexes is higher than in carbonyldiyl complexes. The value of ΔE_{elstat} in the homoleptic complexes is also much higher than the ΔE_{orb} term.

The results of our study can be used to address the controversial interpretations of the TM-ER bond that have been suggested in the literature.³⁶ One controversy concerns the question of whether the iron-gallium bond in (CO)₄Fe-GaAr* should be considered as a triple⁶ or as a single¹⁰ bond. The ETS results clearly show that the π bonding contribution to the (CO)₄Fe-GaPh bond is very small. This suggests that a formula with a single bond is more appropriate. We want to point out, however, that the bonding description of TM-ligand bonds in terms of Lewis structures is not a very good model for the true bonding situation in the compounds. Table 2 shows that the energy contributions of the Fe → CO π back-donation to the bond energy in Fe(CO)₅ is as high as the Fe ← CO σ donation, but writing Fe(CO)₅ with triple bonds between Fe and CO would lead to absurd Lewis structures. The same reasoning holds for Fe(BMe)₅ and Ni(BMe)₄.

The second controversy concerns the question of whether a polar bonding description [(CO)₄Fe]²⁻[AlCp*]²⁺ is appropriate for the electronic structure of (CO)₄Fe-AlCp*. Arguments that have been given in favor of a polar bonding model are based on the short Al–C distances, the observed C–O stretching frequencies, and the calculated atomic partial charges of (CO)₄Fe-AlCp.^{8,36} The ionic model was challenged because the calculated partial charge at the (CO)₄Fe fragment of (CO)₄Fe-AlCp was found to be only -0.75.¹³ The results of the energy

(36) After this paper was submitted, a review by Linti and Schnöckel appeared in which the bonding situation in transition metal complexes with AIR and GaR ligands was discussed (Linti, G.; Schnöckel, H. *Coord. Chem. Rev.* **2000**, 206–207, 285). The authors suggest that force constants should be used for the interpretation of the chemical bond. It is concluded that the (CO)₄Fe-AIR and (CO)₄Fe-CO bonds are similar and should be considered as double bonds. We want to point out that force constants only give information about the strength of the instantaneous interatomic interactions without saying anything about the ionic/covalent contributions and the multiple-bond character. Table 2 shows that the (CO)₄Fe-AlCp and (CO)₄Fe-CO bonds have similar bond strengths and similar covalent characters, but the π contributions to the orbital interactions are very different.

analysis support the conclusion that a polar bonding model is not appropriate for $(\text{CO})_4\text{Fe-AlCp}$, because the energy contributions of ΔE_{elstat} and ΔE_{orb} in the axial isomer are about the same size (Table 2). However, the results presented here show that the atomic partial charges can be misleading and that they are not very helpful for the analysis of the chemical bond. Concerning the use of experimental data for the interpretation of the chemical bond, we refer to a recent paper by Cremer et al.³⁰ which shows that it is very difficult to assign the nature of a chemical bond when only observable quantities are considered. We also point out two papers which showed that the C–O stretching frequencies of carbonyl complexes are influenced not only by the TM \rightarrow CO π back-donation but also by the charge at the metal.³¹ The physical and chemical properties of a molecule are the results of the joint interatomic forces. The correlation of an observed property with a particular component may or may not be justified. The true nature of a chemical bond can only be revealed by the analysis of the different energy contributions (which are not accessible by experimental means) to the interatomic interactions.

6. Summary and Conclusion

The questions which were posed at the end of the Introduction can now be answered as follows: (a) The attractive orbital interactions between Fe and ER in $(\text{CO})_4\text{Fe-ER}$ arise mainly from Fe \rightarrow ER σ donation. A significant contribution by Fe \rightarrow ER π back-donation in $(\text{CO})_4\text{Fe-ER}$ is only found when E is B, but the Fe \leftarrow ER σ donation remains the dominant orbital interaction term. (b) Complexes $(\text{CO})_4\text{Fe-ER}$, where R is a poor π donor, have only slightly stronger Fe \rightarrow ER π back-donation when compared to strong π donor substituents R. (c) Electrostatic interactions and covalent interactions have a similar strength in $(\text{CO})_4\text{Fe-ER}$ complexes when E is Al–Tl and when

R is a good π donor substituent. The Fe–BR bonds of the boron carbonyldiyl complexes have a significantly higher ionic character than the heavier group-13 analogues. Weak π donor substituents R enhance the ionic character of the $(\text{CO})_4\text{Fe-ER}$ bond. The electrostatic interactions arise from the attraction between the negative charge concentration at the overall positively charged donor atom E of the Lewis base ER and the positive charge of the iron nucleus. (d) The TM–E bonds in the homoleptic complexes $\text{Fe}(\text{EMe})_5$ and $\text{Ni}(\text{EMe})_4$ have a stronger ionic character than they do in $(\text{CO})_4\text{FeER}$. The contribution of the TM \rightarrow ER π back-donation to the ΔE_{orb} term is clearly higher in the homoleptic complexes where no other π acceptor ligands are present. (e) CO is a stronger π acceptor than BMe when the two ligands compete with each other, but the relative contribution of the Fe \rightarrow BMe π back-donation to the ΔE_{orb} term in $\text{Fe}(\text{BMe})_5$ is nearly as high as the Fe \rightarrow CO π back-donation in $\text{Fe}(\text{CO})_5$.

Acknowledgment. This work was supported by the Deutsche Forschungsgemeinschaft and the Fonds der Chemischen Industrie. We thank Inga Ganzev for valuable technical assistance. Excellent service by the Hochschulrechenzentrum of the Philipps–Universität Marburg is gratefully acknowledged. Additional computer time was provided by the HLRZ Stuttgart and the HHLRZ Darmstadt.

Supporting Information Available: One table that contains the Cartesian coordinates of the optimized geometries and the energies of the calculated molecules that were calculated at BP86/TZP. This material is available free of charge via the Internet at <http://pubs.acs.org>.

JA002845G